

Flutter Analysis of Tapered Composite Fins: Analysis and Experiment

Mirko Dinulović

Full Professor
University of Belgrade
Faculty of Mechanical Engineering

Boško Rašuo

Full Professor
University of Belgrade
Faculty of Mechanical Engineering

Ana Slavković

Professor
Academy of Applied Technical Studies
Belgrade

Goran Zajić

Professor
Academy of Applied Technical Studies
Belgrade

In the present work, the aeroelastic stability of tapered composite plates is investigated. Existing flutter models, based on the typical section approach, are reviewed for quasi-steady and unsteady low Mach number axial flows and modified for the thin composite tapered plates. The numerical approach, based on panel vortex methods for flutter analysis, is presented, and results are compared to typical section flutter methods for the tapered composite fins. Experimental work is performed in the subsonic wind tunnel at flow speeds of 20 – 30 m/s range. Good agreement between experimental, analytical, and numerical results is obtained, and it was concluded that the presented methodology could be used for estimating the flutter boundary velocities for the composite thin flat plates.

Keywords: *aeroelastic stability, flutter, composites, Mach number, thin composite plates, missile fin.*

1. INTRODUCTION

Mostly because of their intrinsic possibility to be tailored to a specific engineering application, composite materials, in recent years, have gained the interest of many researchers, designers, and industries. Composites are now used as materials of primary choice in many industries, like aerospace, automotive, and construction industries, to name just a few. In the aerospace industry, known for its stringent standards, composite systems are used as the main building block, even in primary aerostructures. By the proper mix of composite system phases, almost any material characteristic (Conductivity, Corrosion Resistance, Density, Ductility, Elasticity/Stiffness, Fracture Toughness, Hardness, Plasticity, Fatigue Strength, Shear Strength, Tensile Strength, Yield Strength, Toughness, etc.) can be designed to meet specific requirements [1-2].

The present paper analyses the bending-torsion flutter of a tapered composite fin. All flying vehicles are built to be light and therefore deform under aerodynamic loading during flight. In turn, these deformations change the loading distribution, which again changes deformations. This interaction may lead to potentially fatal failure of the structure. Flutter is a phenomenon that must be completely prevented from occurring within the flight envelope. Based on this, it is of paramount importance to have reliable methods for flutter predictions of composite structures that can be used in the early stages of the design. In this paper, several flutter prediction methods developed for the isotropic materials are analyzed and modified toward flutter analysis of orthotropic composite laminates, results are compared to known numerical models, and

finally to the results obtained by wind tunnel testing in the subsonic regime [3].

2. BENDING-TORSION FIN FLUTTER ANALYSIS

Flutter analysis ensures the aircraft is free from flutter within the prior defined flight envelope. Flutter tests have to be performed to demonstrate the accuracy of the analyses and prove the flight-worthy structures are safe to operate. Flight flutter tests are required, however, they are dangerous and expensive; on the other hand, many flutter testing nowadays is done in wind tunnels. Flutter testing in wind tunnels requires expensive testing apparatus and relatively long preparation times and mostly because of the high prices of wind tunnel operations' vast economic resources. Bearing these facts in mind, in recent years, methods for flutter velocity estimates have been under constant development and in the focus of many researchers. [4-7]

Methods of flutter analysis can be broadly classified into two categories: analytical (classical) and numerical (certain combined methods also exist). The classical method is usually only used as a first flutter boundary estimate and in the process of initial structural sizing. Due to the limitation of compressibility correction, assumption of lift curve slope, and exclusion of non-linear structure stiffening effects, flutter velocities obtained by these methods can vary up to 40%. Numerical methods of flutter analysis are time marching analysis methods and are more accurate, however, they require high CPU resources, long modeling times, and very often expensive commercial software modules [8-11].

In the present paper, the goal is to present a methodology for the estimation of the composite structure (thin, airfoiled plates) flutter velocity for different flow conditions and relatively small Re numbers. First, the binary (2 DOF) flutter model is analyzed, and one of the objectives was to derive equations of motion of the lifting surface typical section. [12-13].

Received: April 2022, Accepted: August 2022

Correspondence to: Dr Mirko Dinulovic, University of Belgrade, Faculty of Mechanical Engineering, Kraljice Marije 16, 11120 Belgrade 35, Serbia
E-mail: mdinulovic@mas.bg.ac.rs

doi:10.5937/fme2203576D

© Faculty of Mechanical Engineering, Belgrade. All rights reserved

FME Transactions (2022) 50, 576-585 576

The typical section (or sometimes called the characteristic section) is located at 0.70 – 0.75 % semi-span. It is assumed that all required (aerodynamic and structural) characteristics of the lifting surface analyzed can be presented with the same values as for the typical section. The ‘typical section’ lifting surface idealization with binary models (pitch–plunge degrees of freedom) is very effective in flutter analysis and it is possible to perform the unsteady and quasi-steady analysis using different aerodynamic models [14-15]. The typical section method has been analyzed by many authors in recent years, and the methodology is well established; however mostly related to isotropic materials (primarily aluminum) whereas the flutter analysis of composite structures requires further investigation.

The typical section of an airfoiled (thin) fin is presented in Figure 1.

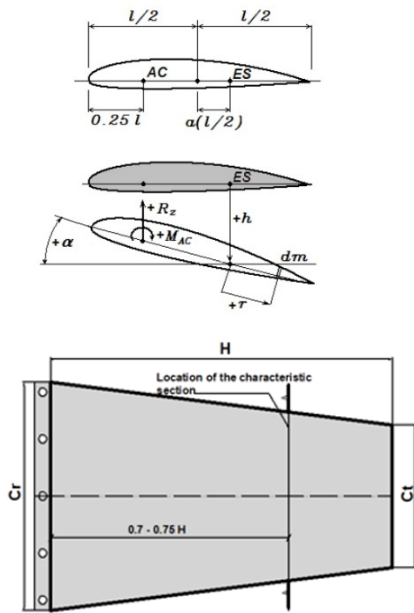


Figure 1. A typical section is located at 0.75 % of the lifting surface span.

In many engineering dynamics analyses [16], the objective is to derive equation(s) of motion of the system analyzed using different methods currently available. For the composite structure analyzed in this work, relations for potential and kinetic energy are written in terms of the selected system’s degrees of freedom (h – plunge and α – twist for the lift surface section, presented in figure 1). It is assumed that the system twists about the shear center (Es), whereas the aerodynamic loading (R_z – Lift force and Mac – aerodynamic moment) acts in the aerodynamic center (ac).

It is assumed in the present analysis that the aerodynamic center is located at the quarter chord (section) span measured from the leading edge. In general, when analyzing thin-walled structures, determination of the section shear center of twist requires separate analysis (analytic or numerical) based on the methods well established in the Elasticity theory of thin structures. The shear center (ES) is a structural feature of the lifting surface; it is a location along the chord such that the acting force causes bending without twisting of the surface. The shear center position depends on the cross-section geometry (for the isotropic

structures, whereas for composites, composite lay-up has a certain degree of influence on shear center location). In the present analysis, the ES location is taken into account through the term $a(l/2)$ where the value of an in the vicinity of 0.2-0.245, which was taken as a reference by performing numerical analyses for the shear center position for NACA 0006 – 0012 airfoil series of an airfoil. A typical section model, the two-degree-of-freedom airfoil system, can give a lot of insights and useful information about the physical aeroelastic phenomena [16-17].

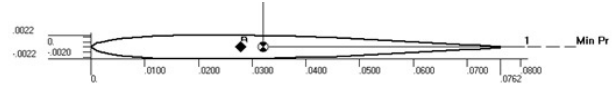


Figure 2. NACA 0006, shear center position

For the two-degree system presented in Figure 1, potential and kinetic energy in terms of plunge (h) and twist (α) are expressed as:

$$E_k = \frac{1}{2} \left(\int dm \right) \dot{h}^2 + \frac{1}{2} \left(\int r dm \right) 2 \dot{h} \dot{\alpha} + \frac{1}{2} \left(\int r^2 dm \right) \dot{\alpha}^2 \quad (1)$$

$$dE_k = \frac{1}{2} \left(\dot{h} + r \dot{\alpha} \right)^2 dm = \frac{1}{2} \left(\dot{h}^2 + 2 \dot{h} r \dot{\alpha} + r^2 \dot{\alpha}^2 \right) dm$$

$$E_p = \frac{1}{2} C_h \cdot h^2 + \frac{1}{2} C_\alpha \cdot \alpha^2 \quad (2)$$

Further, by the introduction of the artificial damping term in the form:

$$D = \frac{1}{2} \frac{g_h C_h \dot{h}^2}{\omega} + \frac{1}{2} \frac{g_\alpha C_\alpha \dot{\alpha}^2}{\omega} \quad (3)$$

and using Lagrange’s equations of the second kind, the typical fin section, equations of motion (2 DOF) are expressed in the following form:

$$\begin{aligned} \ddot{h} + \frac{S_k}{M_k} \ddot{\alpha} + g_h \frac{\omega_h^2}{\omega} \dot{h} + \omega_h^2 h &= - \frac{R_z(t)}{M_k} \\ \ddot{\alpha} + \frac{S_k}{I_k} \ddot{h} + g_\alpha \frac{\omega_\alpha^2}{\omega} \dot{\alpha} + \omega_\alpha^2 \alpha &= \frac{M_T(t)}{I_k} \end{aligned} \quad (4)$$

In the previous equation (eq. 4), $R_z(t)$ and $M_T(t)$ are aerodynamic forces and moments, with artificial damping terms (both structural and fluid) denoted as g_h and g_α , respectively. The natural frequencies of the system oscillation are ω_h and ω_α . Inertial characteristics of the fin section (moments of inertia) are I_k and S_k .

System of equations (eq. 4) represents the equations of motion, for the 2 degrees of freedom fin model in subsonic flows.

Analyzing equations derived, it is obvious that the system’s modal characteristics are required coupled with the adequate aerodynamic theory for the problem analyzed (quasi-steady or unsteady). The applicable aerodynamic theories will be discussed in the subsequent sections.

2.1 Thin plate modal analysis

Required modes of oscillations for the composite systems can be determined in several ways: Analy–

tically, numerically, or using an experimental approach. Analytical methods based on the Rayleigh-Ritz approach are very effective; however, they are generally used for simple systems (isotropic rectangular plates, as an example) [18-20].

The natural frequencies based on the Rayleigh-Ritz method of the thin cantilever plate are:

$$\omega_n = \frac{\lambda_n}{b^2} \sqrt{\frac{D}{\rho \cdot t}} \quad (5)$$

In the previous equation, ρ represents material density, and D is plate flexural rigidity computed from the following relation:

$$D = \frac{E_{eq} \cdot t^3}{12(1-\nu_{eq}^2)} \quad (6)$$

Coefficients λ_n for isotropic materials as a function of taper ratio (tip chord/root chord) are given in Table 1.

Table 1. Coefficients λ_n for isotropic materials

| C_{tip} / C_{root} | Bending | Torsion |
|----------------------|---------|---------|
| 2 | 3.51 | 5.37 |
| 1 | 3.49 | 8.55 |
| 0.5 | 3.47 | 14.90 |

For the composite systems, and based on the FEA approach correction coefficients, the first two modes of oscillations are calculated and presented in figure 3 for the plate aspect ratios 0.5 - 2.

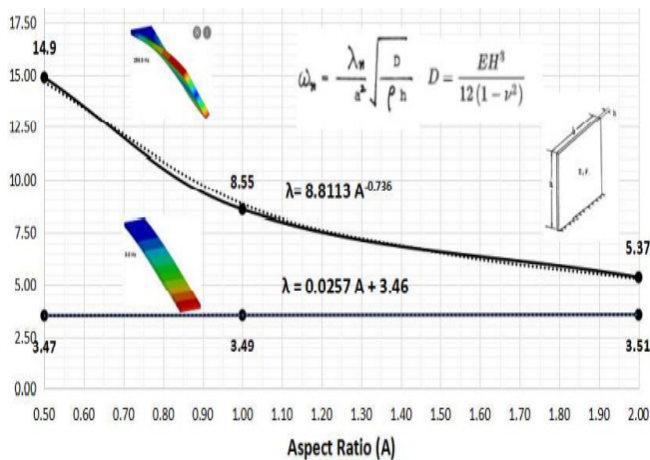


Figure 3. orthotropic correction coefficients

Values of required frequencies (bending and torsion) can also be obtained using the Finite element approach by performing modal analysis. The algorithm for modal extraction used in this example was the complex Lancosz algorithm since it was found that this algorithm for problems of similar size does not miss any modes; it is fairly fast and does not require fine mesh, which can be of importance when several case scenarios have to be analyzed. This was concluded based on the sensitivity analysis performed and results obtained from the experimental modal analysis. Mode shapes for the composite tapered fin analyzed are given in figure 4.

Plate natural frequencies, in bending and twisting (ω_h, ω_a), can be measured experimentally by performing impact testing on the same specimens that are used for

wind tunnel testing at the later experimentation phase. In general, in experimental modal analysis, structures are excited by means of electrodynamic and servohydraulic shakers controlled by a signal generator connected to a power amplifier.

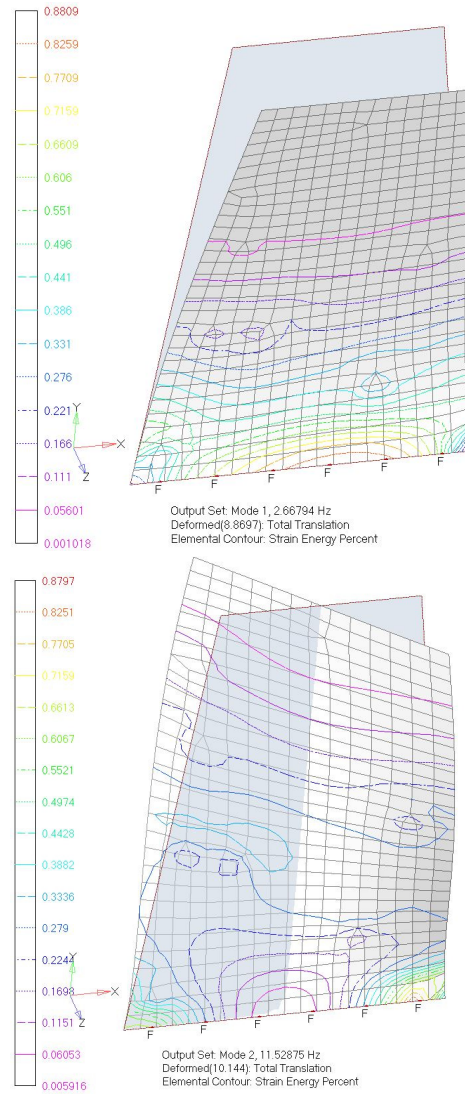


Figure 4. Tapered plate mode shapes

For thin-walled structures more convenient method for structure, excitation is by means of an impact hammer equipped with a piezoelectric force transducer. The modal hammer excites the structure analyzed with a constant force over a frequency range of interest. Initially, this frequency range is not known in order to determine the frequency range for the tapered PLA plates for the first two modes. The system schematics are given in Figure 5, and the Modal results are in Figure 6 and Table 2.

Table 2. Modal results: Mode Indicator - Modal Peaks Function

| Mode | Frequency (Hz) | Damping (%) | Res Mag (m/s ²) | Res Phs |
|------|----------------|-------------|-----------------------------|---------|
| 1 | 3,77 | 1,87 | 344, | 138, |
| 2 | 12,3 | 0,827 | 359, | 307, |
| 3 | 55,2 | 0,812 | 38,7 | 175, |

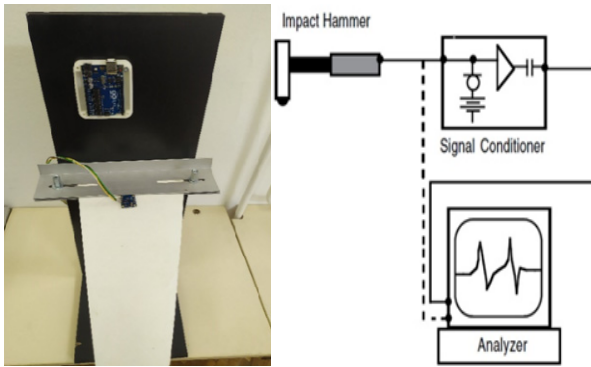


Figure 5. Modal testing system

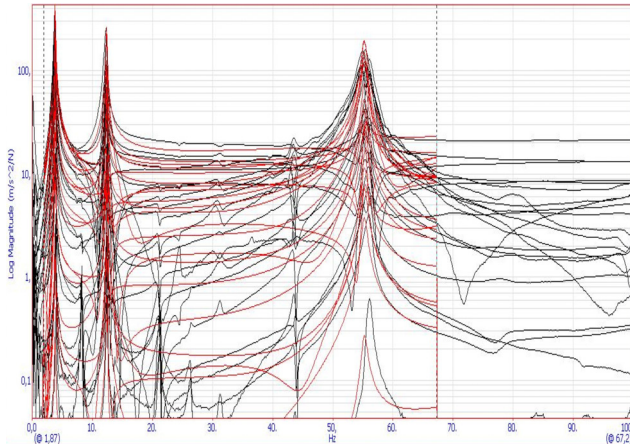


Figure 6. Modal results

2.2 Unsteady aerodynamics model

The solution to the equations of motion requires the choice of aerodynamic theory for the particular problem on hand.

One of the applicable unsteady aerodynamics theories for the flutter analysis is the unsteady Theodorsen theory, which is used throughout this work.

Complex transfer Theodorsen function is the Fourier transform of the unsteady unit air load due to sudden and impulsive plunging motion of the aerofoil, located at the control point in the domain reduced-frequency. The reduced frequency is defined as:

$$k = \frac{\omega \cdot l}{2V_0} \quad (7)$$

whereas the location of the control point is presented in Figure 7.

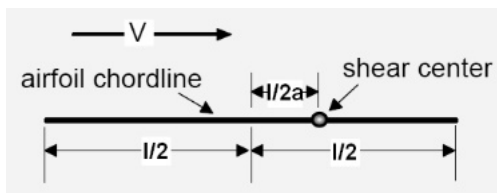


Figure 7. control point location on the airfoil section

Because of the counteracting vorticity that is created in the wake, it presents a lag in the air load from infinitesimal variations of the bound circulation. This approach is very often used in unsteady flutter analysis. Unsteady Aerodynamic force (R_z) and unsteady aerodynamic moment are given in the following form:

$$R_z(t) = \pi\rho \frac{l}{2} V^2 \left\{ \begin{aligned} & \frac{l}{2V^2} \ddot{h} + \frac{2}{V} C(k) \dot{h} - \frac{l^2 a}{4V^2} \ddot{\alpha} + \\ & + [1 + (1-2a)C(k)] \frac{l}{2V} \dot{\alpha} + 2C(k)\alpha \end{aligned} \right\} \quad (8)$$

$$M_T(t) = -\pi\rho \frac{l^2 V^2}{4} \left\{ \begin{aligned} & -\frac{al}{2V^2} \ddot{h} - (1+2a) \frac{1}{V} C(k) \dot{h} + \left(\frac{1}{8} + a^2\right) \frac{l^2}{4V^2} \ddot{\alpha} \\ & - \pi\rho \frac{l^2 V^2}{4} \left\{ \begin{aligned} & -\left[a - \frac{1}{2} + 2\left(\frac{1}{4} - a^2\right)C(k)\right] \frac{l}{2C(k)} \dot{\alpha} - \\ & -(1+2a)C(k)\alpha \end{aligned} \right\} \end{aligned} \right\}$$

A solution to the previous set of equations for the quasi-steady flutter case is obtained by assuming harmonic motion in the following form:

$$\begin{aligned} h &= \bar{h} \cdot \sin(\omega t), \\ \alpha &= \bar{\alpha} \cdot \sin(\omega t) \end{aligned} \quad (9)$$

For the assumed harmonic plate motion, the F and G functions in equation 13 (eq 13) represent the in-phase and out-of-phase components of the Theodorsen Circulation Function $C(k)$. As a function of reduced frequency (k), and are given in the following form:

$$C(k) = F(k) + iG(k) \quad (10)$$

Functions F and G are given in the following form:

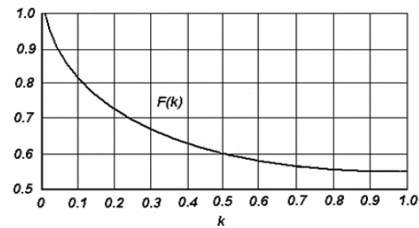


Figure 8. Circulation function real part $F(k)$ as a function of a reduced frequency

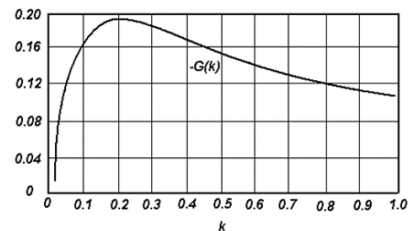


Figure 9. Circulation function real part $G(k)$ as a function of a reduced frequency

The good approximation of the circulation function $C(k)$ (with an error less than 4%) can be expressed as:

$$C(k) = \frac{(1+i10.6k) \cdot (1+i1.774k)}{(1+i3.51k) \cdot (1+i2.745k)} \quad (11)$$

The unsteady flutter solution requires iterative calculations where, usually, structural damping vs. linear velocity for both bending and torsion modes are represented in graphical form. The starting point, using this approach, is to estimate the starting value of the flutter reduced frequency [16-17]. The starting value for the flutter reduced frequency is usually obtained by assuming a quasi-steady flutter case since it is less computationally involved. Based on this value, the Theodorsen aerodynamic functions required in equation 12 (eq. 12) are calculated. Several iterations through the

equations are performed in order to find damping and velocity pairs for particular values of different reduced frequencies (k). When a satisfactory number of data pairs are calculated, graphs for each modal pair of artificial structural damping versus velocity are created. It is required that an adequate number of points exist to construct graphs in order to determine the intersection with the horizontal axis (velocity). That intersection point represents zero damping. At that particular velocity, the loss of stability occurs, and it is considered to be the velocity that corresponds to flutter (V_F)

2.3 Quasi-steady aerodynamics model

In the calculation of varying aerodynamic forces and moments, using the quasi-steady approach, the assumption is that at any instant, airfoil behaves with the characteristics of the same airfoil having the same values of speed and same displacement. Hence, Quasi-steady aerodynamics assumes that forces and moments depend solely on the instantaneous motion of the surface, and the prior history of motion is neglected. The quasi-steady aerodynamic force is expressed as:

$$R_z(t) = -\frac{1}{2} C_{L\alpha} \cdot \alpha(t) \cdot \rho \cdot V_0^2 \cdot c \quad (12)$$

In the previous equation, C_l is the lift coefficient assumed to be the function of the airfoil shape and the angle of attack α .

Using Prandtl-Glauert correction for the lift coefficient, in the form where A is the fin aspect ratio,

$$C_{L\alpha} = \frac{2\pi \cdot A}{2 + \sqrt{A^2 + 4 - \frac{A^2 \cdot V_0^2}{a_0^2}}} \quad (13)$$

The quasi-steady flutter speed can be expressed as:

$$V_F = U(\omega_1 = \omega_2) = \sqrt{\frac{\pi c^2 r_\alpha^2 \mu (\omega_\alpha^2 - \omega_h^2)}{8 C_{L\alpha} x_a}} \quad (14)$$

In relations (6), ω_h and ω_a are the bending and twisting natural frequencies of the plate, r_α is the radius of gyration about the mid-chord, and μ is the dimensionless plate airstream mass ratio.

2.4 Numerical flutter model

The complete fin flutter model consists of a structural model and the aerodynamic model. The structural model consists of 172 laminate finite type finite elements (Classic Lamination Theory) that discretize the complete missile fin domain. The aerodynamic model computes the aerodynamic forces based on the vortex panel method. To ensure the transfer of aerodynamic loading onto fin structure, both models are mutually interconnected with beam-type splines. This kind of flutter model enables analysts to obtain the flutter velocities, hence the fin dynamic stability loss. The algorithm used for this coupled flutter numerical model was a very well-known P-k algorithm [21].

Using Commercial software MSC Nastran/Flight Loads, flutter speed, for the e-glass composite fin, of QI stack up $[0^0/45^0/-45^0/90^0]_s$, thickness 0.65 [mm] is calculated. Geometric dimensions of the fin analyzed are as follows: Root chord, $C_r=180$ [mm], tip chord $C_t=90$ and span $b/2 = 262$ [mm]. The numerical model is presented in Figure 1.

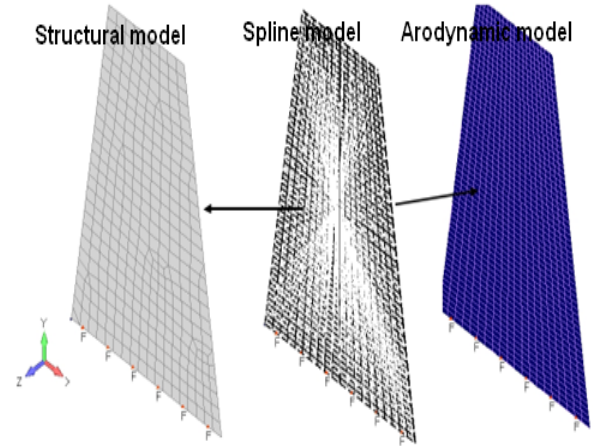


Figure 10. Tapered plate mode shapes

2.5 NACA flutter boundary equation

The national advisory committee for aeronautics, in technical note No 4197, has defined the flutter boundary velocity for the preliminary design of thin plates in the following form:

$$\left(\frac{V_F}{a}\right)^2 = \frac{G_e}{\left(\frac{t}{c}\right)^3 \cdot (A+2)} \cdot \frac{\lambda+1}{2} \cdot \left(\frac{p}{p_0}\right) \quad (15)$$

In the previous equation (Eq. 1), V_f represents flutter boundary speed, a is the speed of sound, G_e is the shear modulus of elasticity, t is the lifting surface average thickness, p/p_0 is the ratio of the fluid pressure to standard pressure, and A and λ are aspect and taper ratio respectively.

Flutter equation (eq.1) for QI laminates reads:

$$V_f = a \cdot \left[\frac{(A+2)}{78.6 \cdot A^3} \cdot \left(\frac{t}{S} \cdot \int_0^{b/2} c(y) \cdot dy \right)^3 \cdot \left(G_{12} + \frac{1}{4} \frac{E_1 \cdot (E_1 + E_2 - 2\nu_{12} E_2)}{E_1 - 2\nu_{12}^2 E_2} \right) \cdot \left(\frac{c_t / c_r + 1}{2} \right) \cdot \left(\frac{p}{p_0} \right) \right]^{1/2} \quad (16)$$

In equation 5, the fin chord (denoted with c in equation 5) is taken as the mean aerodynamic chord for tapered plates and is calculated using the known relation given here for completeness.

$$C_{mac} = \frac{2}{S} \cdot \int_0^{b/2} c(y) \cdot dy \quad (17)$$

$$\left[0^\circ / \frac{180^\circ}{m} \dots (m-1) \frac{180^\circ}{m} \right]_{ns} \quad (21)$$

In equation 2, m represents the number of different orientations in the laminate ($m \geq 3$) and is the number of repetition sequences. This lamination type excludes unfavorable coupling effects and composite (in-plane) stiffness is independent of composite orientation, which may be the main reason why this type of stack-up is often used as the starting point in the early stages of the design. This is of great advantage since the QI stack-up elastic coefficients (principal lamina properties) can be expressed as "equivalent" for the complete laminate, rendering simplification to complex real problem equations (as an example, flutter equation(s) used in this work).

The relations for the laminate elastic coefficients for the QI stack-up are given in the following form:

$$G_{xy} = \frac{1}{2} \cdot G_{12} + \frac{1}{8} \frac{E_1 \cdot (E_1 + E_2 - 2\nu_{12}E_2)}{E_1 - 2\nu_{12}^2E_2} \quad (22)$$

$$E_x = E_y = 2(1 + \nu_{xy}) \cdot G_{xy} \quad (23)$$

The required parameters for the previous set of equations can be obtained from the composite micromechanics as mentioned earlier and are given here for completeness:

$$E_1 = V_f \cdot E_f + V_m \cdot E_m, \quad \nu_{12} = V_f \cdot \nu_f + V_m \cdot \nu_m$$

$$E_2 = \frac{E_m}{1 - \sqrt{V_f} \left(1 - \frac{E_m}{E_2^f} \right)}, \quad G_{12} = \frac{G_m}{1 - \sqrt{V_f} \left(1 - \frac{G_m}{G_{12}^f} \right)} \quad (24)$$

Composite phase properties in previous equations (E_f , E_m , and G_m) are usually obtained from material OEM, data found in the literature, or by experiment. Phases volume fractions (V_f and V_m) are determined by the composite design and are usually within the 55 – 65 [%] range for V_f , for fly-worthy aerospace structural components.

The previously presented approach is applicable to unidirectional laminas (UD), as presented in Figure 12 (A). However, in recent years, the fiber phase can be obtained in the woven form (different weave forms, such as a plain weave), which have certain advantages over UD laminates and are suitable for wet layup processes [23-25]



Figure 12. UD vs. plain weave

In order to determine the laminate equivalent properties of the e-glass epoxy system used in this work, the numerical approach is used based on the lenticular algorithm. The representative volume element (RVE) of

the tapered composite fin manufactured from e-glass/epoxy is presented:

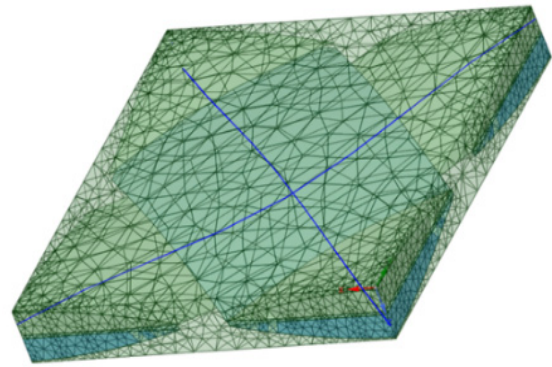


Figure 13. RVE e-glass material model

The commercial software Ansys material designer module is used to determine the equivalent properties of the e-glass/epoxy system, and the obtained numerical results are compared to the OEM components supplier. A good agreement between this material numerical model and phase supplier data is found.

When designing composite structures for flutter, material design and analysis are of great importance, since it does not only affect the overall structure mass but influence the dynamic characteristics of the structure (modal characteristics) which further can affect the overall flutter velocities [26-28].

3. ANALYSIS AND EXPERIMENT

To ensure and verify the validity of the proposed methodology, for the aeroelastic stability of the QI tapered e-glass plates, tests are carried out in the subsonic wind tunnel of the Faculty of Mechanical Engineering, the University of Belgrade, at relatively low Mach number flows (up to 30 m/s), and based on experience and recommendations that were published in paper [29].

A specially designed support structure is used to support the test samples (e-glass tapered fins) and is placed in the test section of the tunnel. Test samples are presented in Figure 14, and the complete test setup (wind tunnel working section) is in Figure 15.

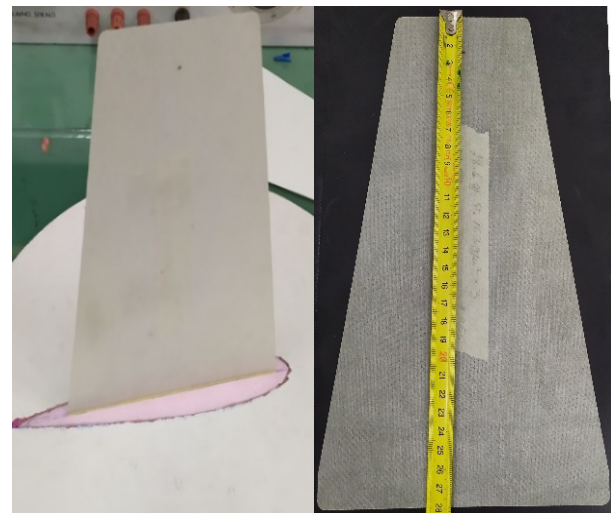


Figure 14. E-glass tapered plate for wind tunnel flutter test



Figure 15. Wind tunnel flutter test setup, 1) Accelerometer (sensor), 2) PCE PFM2 micro manometer with Pitot tube, 3) High-Speed camera(s), 4) Fin testing fixture clamp

The support structure with a clamped sample at the root chord, positioned in the test section of the wind tunnel, is presented in Figure 15. In order to monitor the magnitude of the amplitudes during an oscillation cycle, accelerometers connected to the DAQ system were mounted on the test plate at the location of the root chord. The PCE PFM2 micro manometer with pitot tube is used to determine air-flow velocity. The system can increase or decrease air-flow velocities in the wind tunnel by 0.5 m/s increments, with acceptable air-flow stabilization times.

Table 3. Samples Geometric and material data

| Charact. | |
|------------|---|
| Root chord | 180 [mm] |
| Tip chord | 90 [mm] |
| Span | 262 [mm] |
| thickness | 0.65 [mm] |
| QI | $[0^{\circ}/45^{\circ}/-45^{\circ}/90^{\circ}]_s$ |
| E_1 | 41 000 [MPa] |
| E_2 | 10 400 [MPa] |
| G_{12} | 4300 [MPa] |
| G_E | 7962.59 [MPa] / equation 4 |

The experimental results for flutter velocities versus calculated values based on equation 5 and the numerical model (section 3) for the fin geometry (Table 1) are presented in Table 3. Experimental velocity data is obtained based on 5 fin samples, with 10 runs in the wind tunnel. The flow velocity was gradually increased until the flutter was observed. The flow speed was then reduced to 10 m/s and ramped close to the flow speed where the flutter occurred in the previous run. The loss of stability of the test sample is presented in Figure 16.

Table 4. Flutter velocity comparative results

| Model | Flutter velocity [m/s] |
|---------------|--|
| Experiment | 19.6 – 21.5 / (5 test samples / 10 runs) |
| Quasi-steady | 13.11 |
| Unsteady | 16.78 |
| NACA | 15.3 |
| Numerical P-K | 18.2 |



Figure 16. Wind tunnel flutter test

4. CONCLUSION

In the present work, and based on existing theories, the dynamic stability of tapered e-glass composite plates is investigated. Current quasi-steady and unsteady aerodynamics models were modified in order to predict flutter velocities for low Mach number axial flows. Elastic coefficients for composite materials stiffness matrix are calculated based on Tsai-Ackerman theory and used in flutter and modal analysis. Based on the analysis performed, the following can be concluded:

1. Material characteristics modeling is of great importance when analyzing and designing composite structures for flutter. In cases where weaved phases are used, a numerical approach based on the lenticular algorithm can be deployed with great accuracy.
2. Flutter velocities prediction based on the quasi-steady aerodynamics tend to underestimate flutter speeds (up to 40 % in some cases), however due to their simplicity in engineering application can be used in the preliminary design phase since the underestimation of flutter speed leads to a conservative and safe design.
3. Unsteady aerodynamics requires a lot of modeling effort and computing time; however, it leads to a better solution when results are compared to the experimental results.
4. The closest results obtained to the experimental are based on the numerical model (structure, aero-dynamic, and spline), where the aerodynamic forces are calculated using the panel method approach, using the P-K algorithm.
5. Based on the results obtained, the panel aspect ratio may highly influence the flutter velocities, and this effect requires further investigation.

REFERENCES

- [1] Tsai, S., and Hahn, T.: Introduction to Composite Materials, Lancaster: Technomic, 1980
- [2] Daniel, I. and Ishai, O.: Engineering Mechanics of Composite Materials, 2nd ed., Oxford Press, 2006
- [3] Martin, D.: Summary of flutter experiences as a guide to the preliminary design of lifting surfaces on missiles, NACA TN 4197, 1958.
- [4] Massard, T.: Computer sizing of composite laminates for strength, Journal of Reinforced Plastics and Composites, 3(4), (1984)
- [5] Albano, E., Rodden, W.P.: A Doublet-Lattice Method for calculating lift distributions on oscillating surfaces in subsonic flow, AIAA Journal 7 (2) (1969) 279–285. doi:10.2514/3.5086.
- [6] Kier, T.M.: Comparison of unsteady aerodynamic modelling methodologies with respect to flight loads analysis, in: AIAA Atmospheric Flight Mechanics Conference, AIAA 2005-6027, San Francisco, CA, USA, 2005.
- [7] Lucia, D. J.: The Sensor Craft configurations: A non-linear aeroservoelastic challenge for aviation, in: 46th AIAA/ASME/ASCE/AHS/ASC Structures, Structural Dynamics, and Materials Conference, Austin, TX, United states, 2005, pp. 1768 -1774, AIAA Paper 2005-1943.
- [8] Drela, M.: Integrated simulation model for preliminary aerodynamic, structural, and control-law design of aircraft, in: 40th AIAA Structures, Structural Dynamics and Materials Conference, AIAA 99-1934, St. Louis, MO, USA, 1999, pp. 1644–1656.
- [9] van Schoor, M.C, van Flotow, A.H.: Aeroelastic characteristics of a highly flexible aircraft, Journal of Aircraft 27 (10) (1990) 901–908. doi:10.2514/3.45955.
- [10] Ajaja, R. M. et. al.: Recent developments in the aeroelasticity of morphing aircraft, Progress in Aerospace Sciences, Volume 120, 1 January 2021, 100682, doi. 10.1016/j.paerosci.2020.100682.
- [11] Tiomkina, S., Raveh, D. E.: A review of membrane-wing aeroelasticity, Progress in Aerospace Sciences, Volume 126, 1 October 2021, 100738, doi. 10.1016/j.paerosci.2021.100738.
- [12] Young, D.: Continuous Systems, Handbook of Engineering Mechanics, McGraw-Hill, 1962.
- [13] Baldelli, D.H., Chen, P.C., Panza, J.: Unified aeroelastic and flight dynamic formulation via rational function approximations, Journal of Aircraft 43 (3) (2006) pp. 763–772. doi: 10.2514/1.16620.
- [14] Dowell, E.H. (Editor): A Modern Course in Aeroelasticity, Sixth Edition, Book Series: Solid Mechanics and Its Applications, Volume 264, 2022, Springer Science, Switzerland, doi: 10.1007/978-3-030-74236-2
- [15] Batchelor, G.K.: An Introduction to Fluid Dynamics, Cambridge University Press, 1967.
- [16] Palacios, Murua, R., J., Cook, R.: Structural and aerodynamic models in the nonlinear flight dynamics of very flexible aircraft, AIAA Journal 48 (11) (2010) 2648–2559. doi:10.2514/1.52446
- [17] Murua, J., Palacios, R., Graham, J. M. R.: Assessment of wake-tail interference effects on the dynamics of flexible aircraft, AIAA Journal [Accepted for publication].
- [18] Garinis, D., Dinulovic, M., Rašuo, B.: Dynamic Analysis of Modified Composite Helicopter Blade, FME Transactions, Vol. 40 No 2, 2012, pp 63-68
- [19] K. Maute, M. Nikbay, C. Farhat, Coupled analytical sensitivity analysis and optimization of three-dimensional nonlinear aeroelastic systems, AIAA Journal 39 (11) (2001) 2051–2061. doi:10.2514/2.1227.
- [20] Shearer, C. M., Cesnik, C. E. S.: Nonlinear flight dynamics of very flexible aircraft, Journal of Aircraft 44 (5) (2007) 1528–1545. doi: 10.2514/1.27606.

- [21] Weixing Yuan, Xiaoyang, Z., and Poirel, D.: Flutter Analysis Solution Stabilization for the PK-Method, AIAA Aviation 2021 Forum
- [22] Akkerman, R.: On the properties of quasi-isotropic laminates, Composites: Part B, Vol. 33 (2002) pp. 133-140.
- [23] Dinulović, M., Rašuo, B., Trninić, MR., Adžić, VM.: Numerical Modeling of Nomex Honeycomb Core Composite Plates at Meso Scale Level, FME Transactions, Vol. 48, No. 4, pp. 874-881, 2020,
- [24] Rašuo, B.: Aircraft Production Technology, University of Belgrade, Faculty of mechanical engineering, Belgrade, 1995, (in Serbian).
- [25] Dinulovic, M., Rašuo, B., Krstic, B.: The Analysis of Laminate Lay-Up Effect on the Flutter Speed of Composite Stabilizers, The International Council of the Aeronautical Sciences - The 30th ICAS Congress 25-30. September 2016, Daejeon, Korea, USB Proceedings, pp. 1-6.
- [26] Rašuo, B., Dinulović, M., Free-Edge Stresses in Composite Laminates under Mechanical Loading, 18th International Conference on Composite Materials (ICCM-18), Jeju Island, Korea, August 21-26, 2011, USB-Rom, pp. 1-4.
- [27] Geuzaine, P., Brown, G., Harris, C., Farhat, C.: Aeroelastic dynamic analysis of a full F-16 configuration for various flight conditions, AIAA Journal Vol. 41 (3) (2003) pp. 363-371, doi: 10.2514/2.1975.
- [28] Garcia, J.A.: Numerical investigation of nonlinear aeroelastic effects on flexible high-aspect-ratio wings, Journal of Aircraft 42 (4) (2005) 1025-1036. doi:10.2514/1.6544.
- [29] Očokoljić, G., Damljanović, D., Vuković, Đ., Rašuo, B.: Contemporary Frame of Measurement and Assessment of Wind-Tunnel Flow Quality in a Low-Speed Facility, FME Transactions, Vol. 46, No. 4, pp. 429-442, 2018,

**АНАЛИЗА ФЛАТЕРА КОМПОЗИТНИХ
ТРАПЕЗНИХ РЕПНИХ ПОВРШИНА:
АНАЛИЗА И ЕКСПЕРИМЕНТ**

М. Динуловић, Б. Рашуо, А. Славковић, Г. Зајић

У овом раду се истражује аероеластична стабилност трапезних композитних плоча. Постојећи модели флатера, засновани на типичном приступу пресека, прегледани су за квази-стабилне и несталне аксијалне токове при малим Маховим бројевима и модификовани су за танке композитне трапезне плоче. Приказан је нумерички приступ који је заснован на панел вортекс методама за анализу флатера, а резултати су упоређени са типичним методама флатера пресека за репне површине трапезног облика. Експериментални део рада се изводи у подзвучном аеротунелу при брзинама протока од 20 – 30 м/с. Добија се добра сагласност између добијених експерименталних, аналитичких и нумеричких резултата и закључено је да се приказана методологија може користити за процену граничних брзина лепршања за композитне танке равне плоче.